Ionics (2019) 25:1413–1418
https://doi.org/10.1007/s11581-019-02890-0

SHORT COMMUNICATION

Simple synthesis and electrochemical performance of V_6O_{13} cathode materials as lithium-ion batteries

Xingyu Wu[1] · Zhengguang Zou[1] · Shengyu Li[1] · Zhongwei Wang[1]

Received: 30 November 2018 / Revised: 17 January 2019 / Accepted: 22 January 2019 / Published online: 1 February 2019

Abstract

V_6O_{13} is synthesized by hydrothermal and solvothermal, respectively. The methods are compared to seek a simpler method for V_6O_{13} synthesis. The results show that the best reaction time of hydrothermal-V_6O_{13} is 3.5 h and the phase is pure. Compare with the solvothermal, the hydrothermal-V_6O_{13} has smaller structure unit of about 100–200 nm, and there are also many pores, which is conducive to the transportation and storage of lithium ions. The results of charge-discharge test show that the electrochemical performance of hydrothermal-V_6O_{13} is better than solvothermal-V_6O_{13}. The initial discharge capacity of hydrothermal-V_6O_{13} is 319.2 mAh/g, and the retention rate is 50.5% after 100 cycles, which are 39.9 mAh/g and 12.6% higher than solvothermal-V_6O_{13}, respectively. The results of CV and EIS also confirm that hydrothermal-V_6O_{13} has better electrochemical performance as lithium-ion batteries.

Keywords Lithium-ion batteries · Cathode materials · V_6O_{13} · Hydrothermal

Introduction

With the development of society, the demand of human for energy is increasing. Developing new energy for sustainable development has become an inevitable trend. Energy storage device become a kind of device which can use energy effectively, and lithium-ion batteries are widely used as an energy storage device [1–3]. The cathode material has a great impact on the capacity of lithium-ion batteries [4].

The theoretical specific capacity of traditional cathode materials ($LiCoO_4$, $LiFePO_2$) are relatively low [5, 6]. Vanadium oxides (V_2O_5, V_6O_{13}, VO_2, V_2O_3) [7–11] as cathode materials have higher theoretical specific capacity. In which V_6O_{13} has a kind of double cavity chain structure, which is conducive to intercalation and de-intercalation of lithium ions [12]. The theoretical capacity and theoretical specific energy of V_6O_{13} are 420 mAh/g and 890 Wh/kg at a specific voltage, respectively [13, 14]. Compare with traditional cathode materials, V_6O_{13} has the advantages of high discharge capacity, good thermal stability, and low cost. But V_6O_{13} belongs to metastable state and the valence is between V^{4+} and V^{5+}, so it is difficult to synthesize. The synthetic methods mainly include hydrothermal, solvothermal, sol-gel, and solid-phase method.

Prepared V_6O_{13} by heat treatment of ammonium metavanadate (NH_4VO_3) [15] and it need a long reaction time. Zeng [16] synthesized V_6O_{13} with the morphology of hollow flower by hydrothermal, blending V_2O_5 with H_2O_2 to form sol-gel and adding octylamine and acetone. Its synthesis method is more complicated. Microflower of V_6O_{13} was synthesized by hydrothermal, using ammonium metavanadate (NH_4VO_3) reaction with oxalic acid and lithium nitrate [17]. Li [18] synthesized nanofibers-V_6O_{13} by sol-gel, and it had higher initial discharge capacity, but the capacity decay has exceeded 20% after 20 cycles.

In this work, V_2O_5 and $C_2H_2O_4{\cdot}2H_2O$ were used as raw materials to study the effect of reaction time on the phase by one-step hydrothermal, and the optimum reaction time of V_6O_{13} was determined. V_6O_{13} was synthesized from V_2O_5 and C_2H_5OH by the solvothermal method. The effects of synthetic methods on the morphology and electrochemical performance of V_6O_{13} were investigated. The best synthetic method was determined. Compared with V_6O_{13} prepared by solvothermal method and related literature, it is found that the preparation time of hydrothermal-V_6O_{13} is shorter and the

✉ Zhengguang Zou
zouzgglut@163.com

[1] College of Materials Science and Engineering, Guilin University of Technology, Guilin 541004, China

cost is lower. It has a good electrochemical performance. The contribution of this paper is to optimize the synthesis method and it can provide a reference for the future synthesis of V_6O_{13}.

Experimental

Synthesis route

V_2O_5, $C_2H_2O_4{\cdot}2H_2O$, and C_2H_5OH were used as raw materials. Hydrothermal synthesis of V_6O_{13}: 1 g V_2O_5 and 1.385 g $C_2H_2O_4{\cdot}2H_2O$ were mixed in the reactor lining, then added 50 ml deionized water and stirred at room temperature for 20 min. The product was transferred to the reaction kettle and kept at 170 °C for 1 h, 3.5 h, 6 h, and 8.5 h, respectively. and then the product was centrifuged three times with deionized water, and then freeze-dried at − 50 °C for 24 h. After freeze-dried, the final product was obtained by calcining the product in a nitrogen-protected tubular furnace at 350 °C for 1 h. Solvothermal synthesis of V_6O_{13}: 0.4 g V_2O_5, 25 ml C_2H_5OH, and 20 ml deionized water were stirred in the reactor lining at room temperature for 30 min, transferred to the reaction kettle, and kept at 160 °C for 24 h, repeat the above step of centrifugation and calcination, and obtain the final product.

Characterization

The phase of the products was determined by X-ray powder diffraction (Japan JSM-5610LV). The morphology of the products was characterized by field emission scanning electron microscopy (Hitachi S-4800).

Using X-ray photoelectron spectroscopy (ESCALAB 250Xi) to analyze the composition and valence state of elements. Transmission electron microscope (Philips FEI TECNALG2) was used to observe the nanotopography of samples.

Electrochemical performance measurements

The cathode material, acetylene black, and polyvinylidene fluoride (PVDF) were placed in a mortar at a ratio of 7:2:1, and an appropriate amount of N-methyl pyrrolidone (NMP) was added to make a mixture. It was coated on an aluminum foil and maintained at 90 °C for 12 h with vacuum. A button cell is assembled in the glove box. The charge-discharge tests were performed by a BTS cycler (Shenzhen, China). The cyclic voltammetry (CV) tests and electrochemical impedance spectroscopy (EIS) measurement were characterized by IM6ex electrochemical workstation (Zahner, Germany).

Results and discussion

Figure 1 a is an XRD pattern of hydrothermal-V_6O_{13} and was synthesized at different reaction times. It is not difficult to see that when the reaction time is 1 h, the phases of V_2O_5 and V_4O_9 are present in the product, and the valence of V has a decreasing trend. When the reaction time is 3.5 h, and the diffraction peaks are basically the same as the V_6O_{13} standard card (JCPDF NO.71-2235), which indicates that the synthesized phase is V_6O_{13}. As the reaction time increases, the phase and intensity of the diffraction peak of VO_2 in the product gradually increases. In the process of preparing V_6O_{13} by hydrothermal, the change of the phase can be estimated roughly as $V_2O_5 \rightarrow V_4O_9 \rightarrow V_6O_{13} \rightarrow VO_2$. As the reaction time increases, the reaction time of V_2O_5 in $C_2H_2O_4{\cdot}2H_2O$ is increased and V^{5+} is completely reduced to V^{4+}. Therefore, an appropriate reaction time is advantageous for the synthesis of V_6O_{13}. Fig. 1 b shows the XRD patterns of V_6O_{13} prepared by hydrothermal and solvothermal. It can be seen that the diffraction peaks of the products prepared by the two methods are basically the same. Which are also the same as the V_6O_{13} standard card (JCPDF NO.71-2235), indicating that the synthesized products are V_6O_{13}.

Figure 2 a shows the full spectra of V_6O_{13} prepared by different methods. It can be seen that the composition of V_6O_{13} prepared by different methods is the same, all of which are C 1 s, V 2p, and O 1 s. It indicates that there are elements of O, V, and C in the sample. Figure 2 b–c are narrow spectra in V 2p region of V_6O_{13} prepared by hydrothermal and solvothermal. The peaks of both V $2p_{3/2}$ and V $2p_{1/2}$ were decomposed at 517.1, 516 eV and 524.4, 523.4 eV, corresponding to V^{5+} (524.4, 517.1 eV) and V^{4+} (523.4, 516 eV), respectively [14]. The ratio of V^{4+} and V^{5+} is 2:1, which is consistent with the ratio of V^{4+} and V^{5+} in V_6O_{13}.

Figure 3 a is a SEM image of V_6O_{13} prepared by hydrothermal. It can be seen that the morphology of hydrothermal-V_6O_{13} is composed of irregular thin rods. The thin rod has a width of about 100–200 nm and a length of about 2 μm, and there are many hollow holes in the middle. This structure facilitates the intercalation and de-intercalation of lithium ions, which can shorten the distance and reduce the resistance, and improve the electrochemical performance. Figure 3 b is a SEM image of the product prepared by solvothermal. It can be seen that the morphology is formed by stacking rods of different lengths. The width of the rod is about 300–400 nm and the length is about 1–4 μm. Figure 3 c–d are TEM images of hydrothermal-V_6O_{13} and solvothermal-V_6O_{13}. It can be seen that the width of the hydrothermal-V_6O_{13} is about 150 nm and the solvothermal-V_6O_{13} is about 320 nm, which are consistent with the SEM test results. The increase in the width of the rod influence, the transportation distance of lithium ions, and more resistance need to be overcome during intercalation and de-intercalation. Different synthetic methods cause the

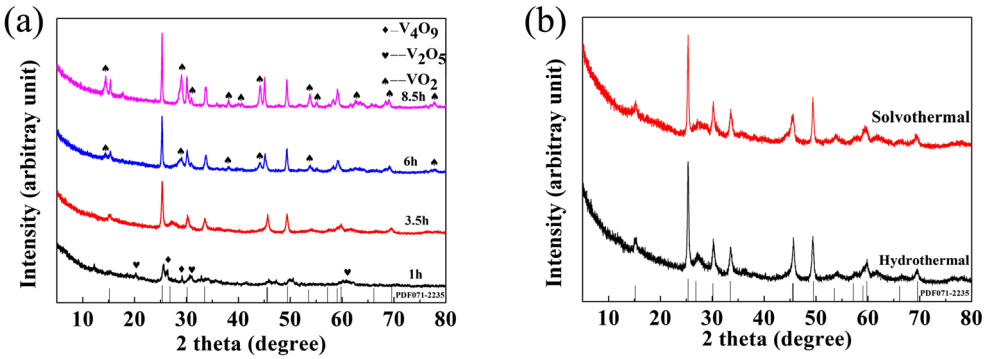

Fig. 1 **a** XRD patterns of V_6O_{13} prepared by hydrothermal at different reaction times, **b** XRD patterns of V_6O_{13} prepared by different methods

morphologies of the product completely different and hydrothermal-V_6O_{13} is more favorable for the electrochemical performance of the material.

Figure 4 a is a charge-discharge diagram of hydrothermal-V_6O_{13} and solvothermal-V_6O_{13} at a discharge rate of 0.1 C (42 mA/g). The first discharge specific capacity of hydrothermal-V_6O_{13} is 319.2 mAh/g, in which the specific capacity and the capacity retention rate are 161.3 mAh/g and 50.5% after 100 cycles, respectively. The first specific discharge capacity of solvothermal-V_6O_{13} is 279.3 mAh/g. The capacity is 106 mAh/g after 100 cycles and the capacity retention rate is 37.9%. By comparison, the hydrothermal-V_6O_{13} is superior to the solvothermal-V_6O_{13} in the first discharge capacity and retention. We can also see that the coulombic efficiency of hydrothermal-V_6O_{13} is 97%, which is higher than that of solvothermal-V_6O_{13}. The reason may be that the morphology of hydrothermal-V_6O_{13} has a small particle size and a large number of hollow holes in the middle, which are advantageous for the intercalation and de-intercalation of lithium ions. And it can also make the material better contact with conductive agent. Figure 4 b is a graph showing the rate performance of hydrothermal-V_6O_{13} and solvothermal-V_6O_{13} at discharge rates of 0.1, 0.2, 0.5, and 1 C. It can be seen that with the increase of the discharge rate, the discharge specific capacity of V_6O_{13} decreases, and when the discharge rate changes back to 0.1 C, the discharge specific capacity of the material is

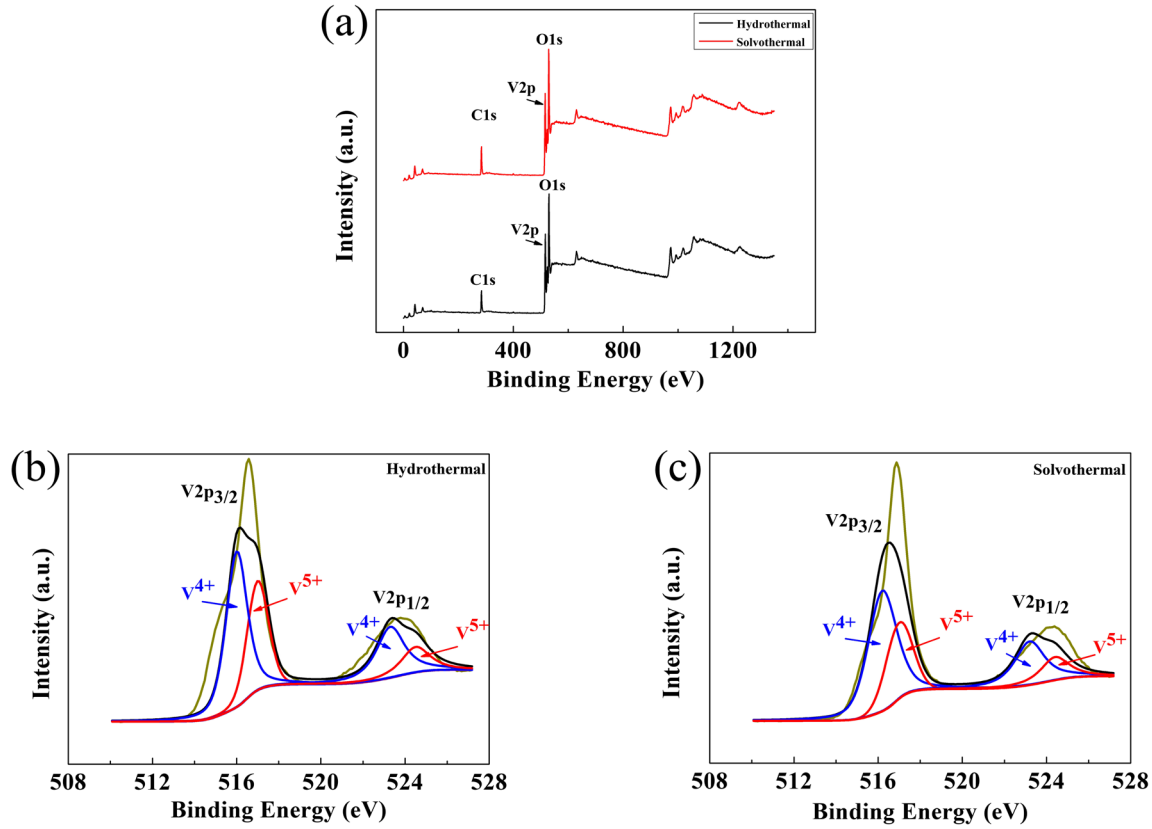

Fig. 2 **a** The XPS survey spectra of V_6O_{13} prepared by different methods, **b** XPS spectrum of V 2p region of hydrothermal-V_6O_{13}, **c** XPS spectrum of V 2p region of solvothermal-V_6O_{13}

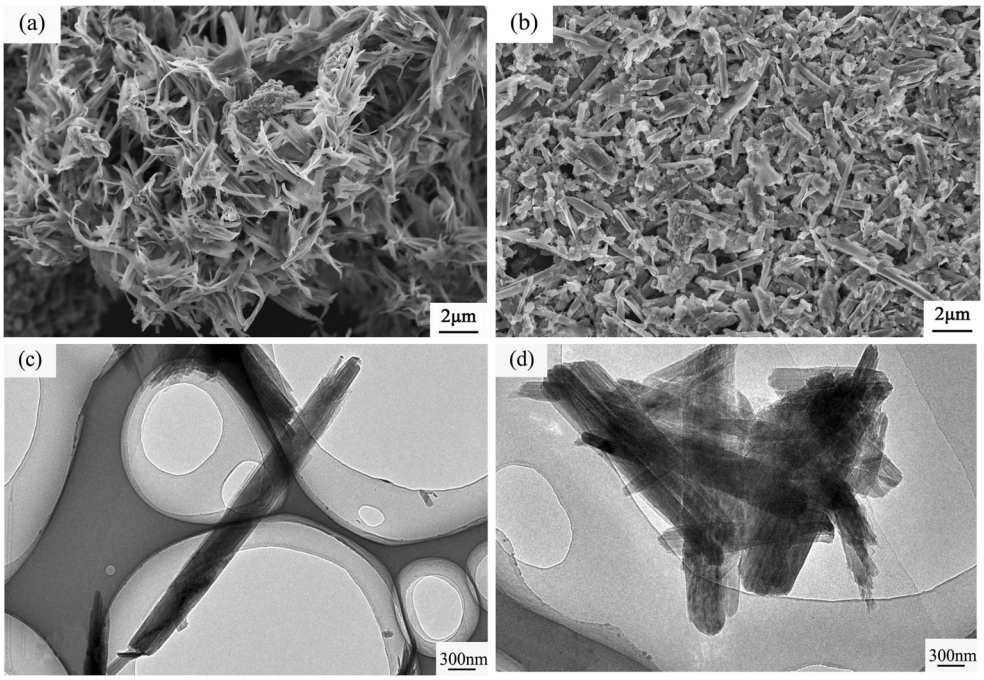

Fig. 3 **a** SEM image of hydrothermal-V_6O_{13}, **b** SEM image of solvothermal-V_6O_{13}, **c** TEM image of hydrothermal-V_6O_{13}, **d** TEM image of solvothermal-V_6O_{13}

improved compared with 1 C. Indicating that the V_6O_{13} shows poor electrochemical performance at large discharge rates. Comparing with the charge-discharge curves of V_6O_{13} prepared by the two methods, the capacity of hydrothermal-V_6O_{13} is always better than solvothermal-V_6O_{13}, which is also the same as the result of 100 charge-discharge cycle tests. The hydrothermal-V_6O_{13} has excellent electrochemical performance than the solvothermal-V_6O_{13}.

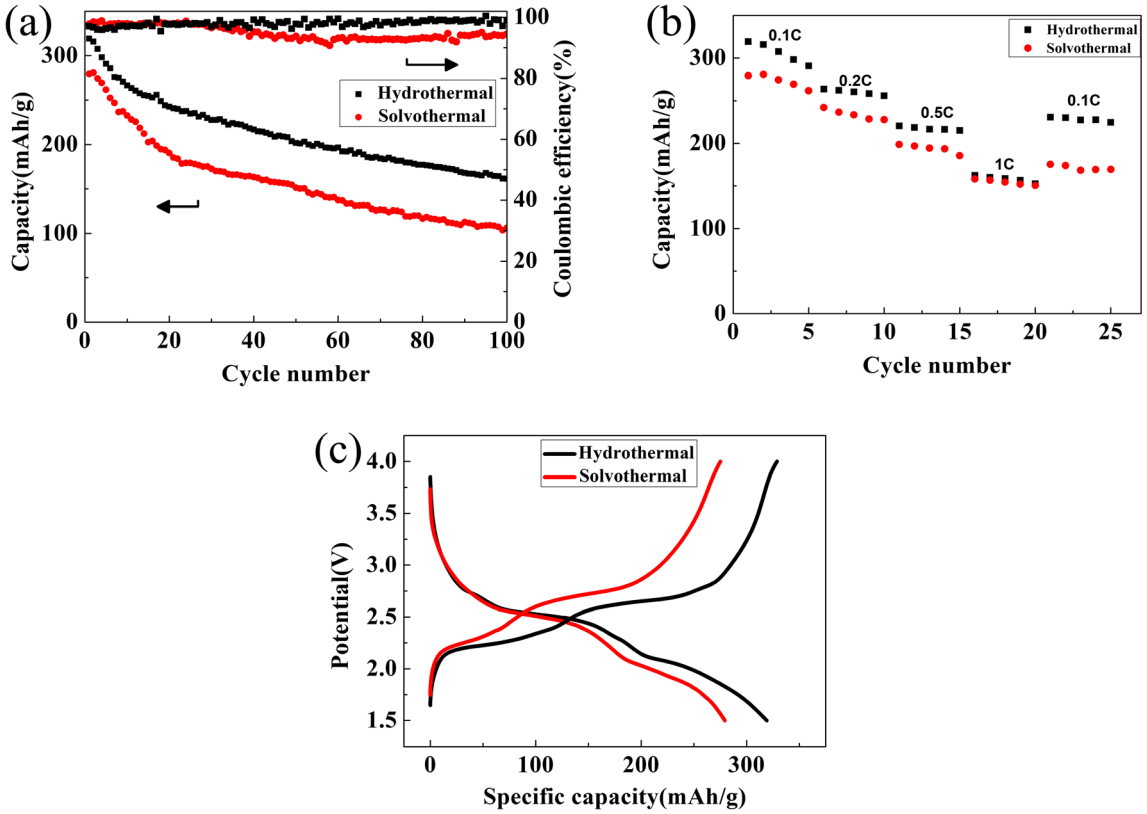

Fig. 4 **a** The cyclic performance and coulombic efficiency of V_6O_{13} prepared by different methods, **b** rate performance of V_6O_{13} prepared by different methods, **c** first charge and discharge curve of V_6O_{13} prepared by different methods

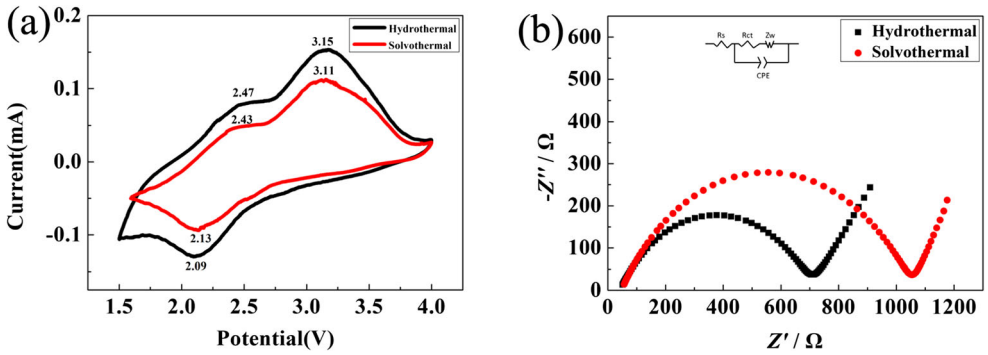

Fig. 5 **a** CV diagram of V_6O_{13} prepared by different methods, **b** EIS diagram of V_6O_{13} prepared by different methods

Figure 4 c is a graph of the first charge-discharge curves of V_6O_{13} prepared by different methods at 0.1 C. It can be seen that each sample has two charging platforms and discharge platforms. The charge and discharge platform represent the phase transition in the material. The discharge platform is at the position of 2.53 V and 2.02 V, which the reduction reaction occurs in V_6O_{13} ($V^{5+} \rightarrow V^{4+} \rightarrow V^{3+}$). The charging platform is about 2.68 V and 2.21 V, and the oxidation reaction occurs ($V^{3+} \rightarrow V^{4+} \rightarrow V^{5+}$). It indicates that the reaction is reversible. The voltage platform of hydrothermal-V_6O_{13} is longer than solvothermal-V_6O_{13}, and the length of the voltage platform is related to the redox reaction kinetics and the reversibility of the system [19]. It indicates that hydrothermal-V_6O_{13} is more reversible.

Figure 5 a is a CV diagram of V_6O_{13} prepared by different methods after three charge-discharge cycles, the voltage range is 1.5–4.0 V, and the scanning speed is 0.1 mV/s. It can be seen from the figure that the CV curves of V_6O_{13} prepared by the two methods are basically the same, and there are a relatively obvious reduction peak and oxidation peak, which reflects the intercalation and de-intercalation of lithium ions. The oxidation peak and reduction peak of hydrothermal-V_6O_{13} are 2.47 V, 3.15 V, and 2.09 V, respectively. The oxidation peak and reduction peak of solvothermal-V_6O_{13} are 2.43 V, 3.11 V, and 2.13 V, respectively. It matches the voltage platform of charge and discharge. The area of oxidation peak and reduction peak reflects the cyclic active substance in the sample. It is obvious that the area of CV curve of hydrothermal-V_6O_{13} is much larger than solvothermal-V_6O_{13}, indicating that there are more cyclic active substances. Figure 5 b shows the EIS pattern of V_6O_{13} prepared by different methods. The semicircle in the high-frequency region represents the charge shift resistance, and the oblique line in the low-frequency region reflects the diffusivity of lithium ions. After Zview software fitting, the charge transfer resistance of hydrothermal-V_6O_{13} and solvothermal-V_6O_{13} is 625 Ω and 1010 Ω, respectively. The charge shift resistance of hydrothermal-V_6O_{13} is small, indicating that lithium ions are more easily remove from V_6O_{13}, which are also because of small size and hollow pores.

Conclusion

In this paper, V_6O_{13} was synthesized by hydrothermal and solvothermal, respectively. The results show that the pure V_6O_{13} is synthesized by hydrothermal with reaction time of 3.5 h. The electrochemical performance of hydrothermal-V_6O_{13} is better than that of solvothermal-V_6O_{13}. The hydrothermal-V_6O_{13} consists of thin rods with hollow holes in the middle, which is beneficial to the transportation and storage of lithium ions in V_6O_{13}. This morphology can also increase the contact between materials and conductive agents, and improving the electrochemical performance. The results of charge-discharge test show that the initial discharge capacity of hydrothermal-V_6O_{13} is 319.2 mAh/g, the discharge capacity is 161.3 mAh/g after 100 cycles and the capacity retention rate is 50.5%, which are higher than that of solvothermal-V_6O_{13}. The curves of CV and EIS further proved that the hydrothermal-V_6O_{13} has more active substances and less resistance. The hydrothermal-V_6O_{13} is not only shorten in synthetic time but also has good electrochemical performance. The purpose of this paper is to research a simple method to synthesize V_6O_{13} and provide a reference for the future synthesis of V_6O_{13}. In the future work, some metal ions will be doped on the hydrothermal-V_6O_{13} and improve the electrochemical performance of V_6O_{13}.

Acknowledgements This work was supported by the National Natural Science Foundation of China (No. 51562006).

References

1. Whittingham MS (1976) Electrical energy storage and intercalation chemistry. Science 192:1126–1127

2. Chen J, Tao ZL, Yuan HT (2007) Research progress on electrode materials for lithium ion secondary batteries. Power technology 131:946–950
3. Li H (2015) Fundamental scientific aspects of lithium ion batteries (XV)—summary and outlook. Energy Storage Science and Technology 4:306–318
4. Li W, Tian WH, Qi L (2015) Technology research progress of cathode material of lithium ion battery. Inorganic chemicals industry 47:1–5
5. Kang K, Meng YS, Breger J, Grey CP, Ceder G (2006) Electrodes with high power and high capacity for rechargeable lithium batteries. Science 311:977–980
6. Wang JJ, Sun XL (2012) Understanding and recent development of carbon coating on $LiFePO_4$ cathode materials for lithium-ion batteries. Energy Environ Sci 5:5163–5185
7. Li XL, Chen XJ, Chen XY, Han CL, Shi CW (2007) Hydrothermal synthesis and characterization of VO_2 (B) nanorods array. J Cryst Growth 309:43–47
8. Mai LQ, Wei QL, An QY, Tian XC, Zhao YL, Xu X, Xu L, Chang L, Zhang QJ (2013) Nanoscroll buffered hybrid nanostructural VO_2 (B) cathodes for high-rate and long-life lithium storage. Adv Mater 25:2969–2973
9. Dellnas C, Cognacallradou H, Cocciantelli JM, Menetrier M, Doumerc JP (1994) The $Li_xV_2O_5$ system: an overview of the structure modifications induced by lithium intercalation. Solid State Ionics 69:257–264
10. BJÖRK H, Sven L, Gustafsson T, Thomas JO (2001) Superlattice formation in thelithiated vanadium oxide phases $Li_{0.67}V_6O_{13}$ and LiV_6O_{13}. Acta Crystallogr B 57:759–765
11. Tan SS, Jiang YL, Wei QL, Huang QM, Dai YH, Xiong FY, Li QD, An QY, Xu X, Zhu ZZ, Bai XD, Mai LQ (2018) Multidimensional synergistic nanoarchitecture exhibiting highly stable and ultrafast sodium-ion storage. Adv Mater 30:1707122
12. Zou ZG, Yuan Q, Wang JL, Gao Y, Wu Y, Long F, Han SC, Wan ZD (2017) Hydrothermal synthesis of high specific capacity Al-doped V_6O_{13} cathode material for lithium-ion battery. Int J Electrochem Sci 12:1670–1679
13. Ding N, Feng XY, Liu SH, Xu J, Fang X, Lieberwirth I, Chen C (2009) High capacity and excellent cyclability of vanadium (IV) oxide in lithium battery applications. Electrochem Commun 11: 538–541
14. West K, Zachau-Christiansen B, Acobsen J, Atlung S (1985) V_6O_{13} as cathode material for lithium cells. J Power Sources 14:235–245
15. Yu DY, Qiu WH, Liu QG, Yang LL, Qiu B (1992) Cyclic voltammetric characteristics of V_6O_{13} electrode in room temperature solid state lithium battery. Chemistry Bulletin 7:30–31
16. Huang ZY, Zeng HM, Xue L, Zhou XG, Zhao Y, Lai QY (2011) Synthesis of vanadium oxide, V_6O_{13} hollow-flowers materials and their application in electrochemical supercapacitors. J Alloy Compd 509:10080–10085
17. Fei HL, Lin YS, Wei MD (2014) Facile synthesis of V_6O_{13} microflowers for Li-ion and Na-ion battery cathodes with good cycling performance. J Colloid Interf Sci 425:1–4
18. Li HQ, He P, Wang YG, Hosono EJ, Zhou HS (2011) High-surface vanadium oxides with large capacities for lithium-ion batteries: from hydrated aerogel to nanocrystalline VO_2(B), V_6O_{13} and V_2O_5. J Mater Chem 21:10999–11009
19. Juan B, Tony J, Markus K, Steffen O, Jürgen E, Lars G (2015) Functional mesoporous carbon-coated separator for long-life, high-energy lithium–sulfur batteries. Adv Funct Mater 25:5285–5291